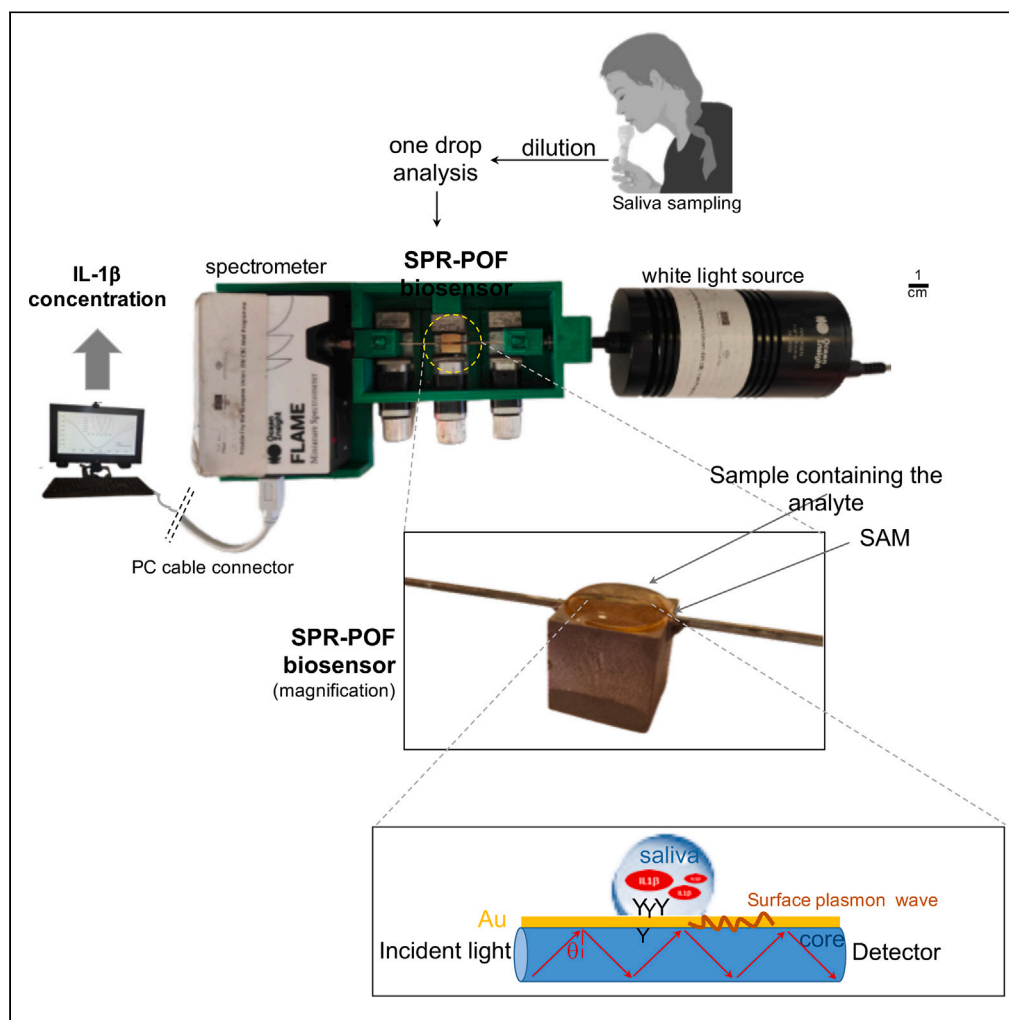


## Article

Plasmon resonance biosensor for interleukin-1 $\beta$  point-of-care determination: A tool for early periodontitis diagnosis

Nunzio Cennamo,  
Debora  
Bencivenga,  
Marco Annunziata,  
..., Luigi Zeni, Luigi  
Guida, Adriana  
Borriello

adriana.borriello@unicampania.it (A.B.)  
luigi.guida@unicampania.it (L.G.)  
luigi.zeni@unicampania.it (L.Z.)

**Highlights**

SPR and antibody-embedded surface are used to develop a portable IL-1 $\beta$  biosensor

LoD in the picomolar range, short time of analysis, high selectivity are demonstrated

Clinically relevant IL-1 $\beta$  concentration can be detected in complex real matrices

The developed biosensor can support early detection of oral inflammatory pathologies

Cennamo et al., iScience 27, 108741  
January 19, 2024 © 2023 The Authors.  
<https://doi.org/10.1016/j.isci.2023.108741>

## Article

Plasmon resonance biosensor for interleukin-1 $\beta$  point-of-care determination: A tool for early periodontitis diagnosis

Nunzio Cennamo,<sup>1,4</sup> Debora Bencivenga,<sup>2,4</sup> Marco Annunziata,<sup>3</sup> Francesco Arcadio,<sup>1</sup> Emanuela Stampone,<sup>2</sup> Angelantonio Piccirillo,<sup>3</sup> Fulvio Della Ragione,<sup>2</sup> Luigi Zeni,<sup>1,\*</sup> Luigi Guida,<sup>3,\*</sup> and Adriana Borriello<sup>2,5,\*</sup>

## SUMMARY

**Among pro-inflammatory cytokines, Interleukin-1 $\beta$  is crucially involved in several inflammatory-based diseases and even cancer. Increased Interleukin-1 $\beta$  levels in oral fluids have been proposed as an early marker of periodontitis, a broadly diffused chronic inflammatory condition of periodontal-supporting tissues, leading eventually to tooth loss. We describe the development of a portable surface-plasmon-resonance-based optical fiber probe suitably coated with an anti-Interleukin-1 $\beta$  antibody monolayer. A picomolar linear range of determination was obtained in both buffer solution and saliva with a rapid (3 min) incubation and high selectivity in presence of interferents. Higher Interleukin-1 $\beta$  concentration in the saliva of a periodontitis patient compared to a healthy control was determined. These measurements were validated by an automated ELISA system. Our results sustain the potential applicability of the proposed SPR-POF as diagnostic point-of-care device for real-time monitoring of salivary Interleukin-1 $\beta$ , that can support early detection of oral inflammatory-based pathologies and rapid and timely therapeutic decisions.**

## INTRODUCTION

Cytokines are important protein mediators that supervise and regulate immune response and inflammation and act as biomarkers for many local and systemic disorders. Consequently, their quantitation has important repercussions in clinical medicine and biology, giving knowledge about both physiological and pathological processes and helping to improve diagnosis and therapeutic approaches.

Among cytokines, the Interleukin-1 (IL-1) family is a group of 11 soluble proteins, including 7 proinflammatory or pyrogenic cytokines (IL-1 $\alpha$  and -1 $\beta$ , -18, -33, -36 $\alpha$ , -36 $\beta$  and 36 $\gamma$ ) and four antagonists or putative antagonists (IL-1Ra, IL-36Ra, IL-37, and IL-38).<sup>1</sup> Prevalently, they play essential roles in triggering and maintaining the host inflammatory response to infection and injury, and act as a bridge between innate and adaptive immune responses.<sup>2</sup> Mechanistically, IL-1 cytokines bind their receptors activating host defense mechanisms such as phagocytosis and degranulation. In addition, they stimulate T and B lymphocyte functions implicated in adaptive immunity. Some IL-1 cytokines, like IL-1 $\alpha$  (structurally related to IL-1 $\beta$ , but with weaker activity) and IL-33 are dual-functioning cytokines, being secreted by different cell types (as the majority of cytokines) and/or acting in the cells where they translocate into the nucleus and induce the expression of leukocyte adhesion molecules and many genes associated with inflammation, i.e., cyclooxygenase-2, type 2 phospholipase A, and inducible nitric oxide synthase.<sup>3,4</sup>

IL-1 $\beta$  is mainly produced by activated monocytes, macrophages, and dendritic cells.<sup>4,5</sup> However, many other cell types can produce it, T-lymphocytes and Natural Killer cells, epithelial cells, fibroblasts, and osteoblasts, among others. It is synthesized as a pro-cytokine of 31 kDa that is cleaved by caspase-1 to generate the mature and active form of 17 kDa.<sup>6</sup> On its side, caspase-1 is activated by multiprotein complexes known as "inflammasomes" whose functions are to sense and react to microbial infection and cellular damage.<sup>7</sup> First identified as a pyrogenic factor, IL-1 $\beta$  has been considered a catabolic protein that induces, in different cell types, the expression of several proteolytic enzymes, such as collagenase, matrix metalloproteinases, and plasminogen, thus contributing to tissue destruction.<sup>8</sup> IL-1 $\beta$ , together with IL-1 $\alpha$ , exerts peculiar and important roles in bone metabolism by enhancing osteoclast formation and differentiation and inducing the expression of RANKL in osteoblasts.<sup>9,10</sup> Accordingly, IL-1 $\alpha/\beta$  KO mice, in particular, showed increased bone mass formation, whereas osteoclasts from IL-1 $\alpha/\beta$  KO animals were unable to resorb bone normally.<sup>10–12</sup> Due to these findings, both IL-1 $\alpha$  and IL-1 $\beta$  have been defined as "clastokines".

<sup>1</sup>Department of Engineering, University of Campania "Luigi Vanvitelli", Via Roma, 9, Aversa, CE 81031, Italy

<sup>2</sup>Department of Precision Medicine, University of Campania "Luigi Vanvitelli", via De Crecchio, 7 80138 Naples, Italy

<sup>3</sup>Multidisciplinary Department of Medical-Surgical and Dental Specialties, University of Campania "Luigi Vanvitelli", via De Crecchio, 6 80138 Naples, Italy

<sup>4</sup>These authors contributed equally

<sup>5</sup>Lead contact

\*Correspondence: [adriana.borriello@unicampania.it](mailto:adriana.borriello@unicampania.it) (A.B.), [luigi.guida@unicampania.it](mailto:luigi.guida@unicampania.it) (L.G.), [luigi.zeni@unicampania.it](mailto:luigi.zeni@unicampania.it) (L.Z.)

<https://doi.org/10.1016/j.isci.2023.108741>



IL-1 $\beta$  levels increase in several inflammatory-based diseases. The cytokine has been proposed as a biomarker of rheumatoid arthritis,<sup>13</sup> allergic rhinitis,<sup>14</sup> and several types of cancer like breast and lung tumors.<sup>15,16</sup> The increase of IL-1 $\beta$  in biological fluids also correlates with negative prognosis in both cancer patients and experimental tumor models since it promotes tumor development, angiogenesis, and metastasis.<sup>17,18</sup>

In the oral cavity, the secretion, induced by pathogenic bacteria, of IL-1 $\beta$  by dendritic cells, macrophages, periodontal fibroblasts, osteoblasts, and ligament cells, activates a cascade of events leading to the spreading of inflammation in soft tissues,<sup>19</sup> periodontal tissue destruction, and alveolar bone resorption, thus participating in the early development and progression of periodontitis<sup>20</sup> and peri-implant diseases.<sup>21</sup> In addition, it has been reported that oral pathogens can produce enzymes that are able to degrade cytokines except IL-1 $\beta$ , resulting in further promotion of osteoclastogenesis.<sup>22</sup>

Periodontitis is a chronic inflammatory disease caused by oral dysbiosis, with consequent inflammatory and host immune response, characterized by periodontal attachment loss and, eventually, tooth loss, mostly in older people.<sup>23</sup> Due to its widespread prevalence and disabling complications, periodontitis is one of the major public health issues in the oral field.<sup>24</sup> Scientific evidence shows that periodontitis is correlated with a range of systemic diseases, including adverse pregnancy outcomes, diabetes, cardiovascular diseases, and even cancer.<sup>25–31</sup>

Periodontitis is currently diagnosed mostly through clinical investigations; the assessment of probing depth, clinical attachment level, plaque index, bleeding on probing, and radiographic findings are the major traditional measures. Unfortunately, being applicable only when visual signs of periodontal tissue destruction appear, and requiring long turn-around times, this approach results in an often-delayed diagnosis and late therapeutic interventions that aggravate the condition.

Oral fluids (saliva and gingival crevicular fluid, GCF) contain specific biomolecules secreted not only in the cases of oral but also systemic inflammatory-based diseases.<sup>32,33</sup> Saliva, in particular, has recently attracted great interest as a noninvasive and easy-to-collect biofluid, in certain cases preferable to blood for detection of biomarkers of local and/or systemic conditions.<sup>34</sup> Several reports listed periodontium diseases' biomarkers detectable in saliva and GCF, categorized as: (1) markers of soft tissue inflammation; (2) markers of alveolar bone loss; and (3) markers (products) of collagen breakdown. Their accurate qualitative and quantitative detection represent a useful tool for disease diagnosis and staging, the identification of the current disease activity, the prediction of its progression, and the monitoring of the therapeutic intervention efficacy.<sup>32,33</sup> Among them, IL-1 $\beta$  has been suggested as an early and precocious biomarker of periodontitis, being one of the primary host response factors linked to the bacterial infection and to development and progression of the disease.<sup>35–40</sup> It is now widely accepted that IL-1 $\beta$  increases in GCF, saliva, and periodontal tissues of periodontitis patients (proportionally to the severity of the disease),<sup>41–44</sup> however its precise concentrations in healthy and pathological conditions have not been univocally defined. In particular, IL-1 $\beta$  concentrations in healthy and periodontitis (stage  $\geq$  II) saliva samples, determined by immunoassay, were reported as  $7.24 \pm 7.69$  (0.43 pM) and  $90.94 \pm 85.22$  pg/mL (5.35 pM), respectively,<sup>45</sup> although a large variability among the salivary IL-1 $\beta$  measurements, particularly for healthy saliva samples, was registered. In the same study, it was shown that panels of analytes (such as IL-1 $\beta$ , IL-6, MMP-8) were able to increase the sensitivity and specificity of the method, distinguishing health from gingivitis and periodontitis. According to a 2015 study, IL-1 $\beta$  concentrations were considerably increased in the periodontitis population ( $102.3 \pm 10.1$  pg/mL  $\equiv$  6 pM) in comparison to gingivitis ( $28.7 \pm 7.3$  pg/mL  $\equiv$  1.7 pM) and healthy ( $14.6 \pm 2.6$  pg/mL  $\equiv$  0.86 pM) participants.<sup>46</sup> By similar analytical technologies, different concentrations were reported, with 94.55 and 216.98 pg/mL (5.56 and 12.76 pM) in healthy and periodontitis samples, respectively.<sup>47</sup> In this reported study, the subjects chewed paraffin wax to favor the collection of "irritant-provoked" saliva.<sup>47</sup> Conclusively, the lack of precise disease staging in the enrolled patients and standardized sampling procedures makes it difficult to compare the results of different laboratories<sup>48</sup> and does not allow for extrapolating ranges of IL-1 $\beta$  concentrations for healthy or pathological conditions. Very recently, Relvas' group<sup>49</sup> demonstrated that salivary IL-1 $\beta$  amount positively correlates with the pocket depth and clinical attachment loss (CAL) indices. Importantly, the salivary IL-1 $\beta$ , together with IL-17A, RANK-L, and OPG, levels enable to differentiate between the incipient and the more advanced periodontitis and, in turn, to discriminate between mild and severe periodontitis conditions,<sup>49</sup> in agreement with the current classification criteria for periodontal diseases.<sup>50</sup> In this observational study, using the spitting method for saliva collection, IL-1 $\beta$  concentrations, measured through immunoassays, were  $913.25 \pm 418.20$  pg/mL ( $\sim$ 53.7 pM),  $1429.38 \pm 1037.22$  pg/mL ( $\sim$ 84.1 pM), and  $1866.25 \pm 1152.15$  pg/mL ( $\sim$ 109.8 pM) in healthy individuals, in stages I/II, and stages III/IV of periodontitis, respectively.<sup>49</sup> Despite the correctness of the reported methodologies, the small gap between the mean values and standard deviations for the quantitative IL-1 $\beta$  determination implies substantial variability, suggesting that major efforts are needed to determine the precise IL-1 $\beta$  levels in healthy and pathological saliva.

As mentioned in the above-reported studies, IL-1 $\beta$  detection was performed mainly by the enzyme-linked immunosorbent assay (ELISA), so far the most sensitive and accurate technique applied for cytokine determination, with an average limit of detection (LoD) of 0.2 pg/mL (0.012 pM).<sup>51</sup> The major drawbacks of ELISA are, however, the relatively long sample processing time and the high costs, which make the method laborious and unsuitable for a rapid out-patient medical diagnosis. On the other hand, an optimal disease diagnostic method should identify the condition before tissue damage is active and clinically relevant signs become detectable. This could be obtained by measuring/following the levels of early disease biomarkers such as IL-1 $\beta$  through highly sensitive point-of-care technologies for a real-time diagnosis and monitoring of the pathology.

Several alternative methods have been proposed for the point-of-care/chair-side detection of IL-1 $\beta$ . The most exploited techniques are surface plasmon resonance (SPR) (gold nanoparticles, modified AuNPs optical fiber/anti-IL-1 $\beta$ ),<sup>52</sup> amperometry (4-carboxyphenyl-functionalized double-walled carbon nanotubes),<sup>53</sup> differential pulse voltammetry,<sup>54</sup> and electrochemical impedance spectroscopy (IES).<sup>55–58</sup> Table S1 lists some IL-1 $\beta$ -detecting biosensors along with their key features. To date, besides the low limits of detection reached by some chips (from 0.008 to 0.2 pg/mL or 0,00048–0.12 pM), the proposed biosensing systems might not completely meet all the criteria for a point-of-care technology, according to the World Health Organization (WHO).<sup>59</sup>

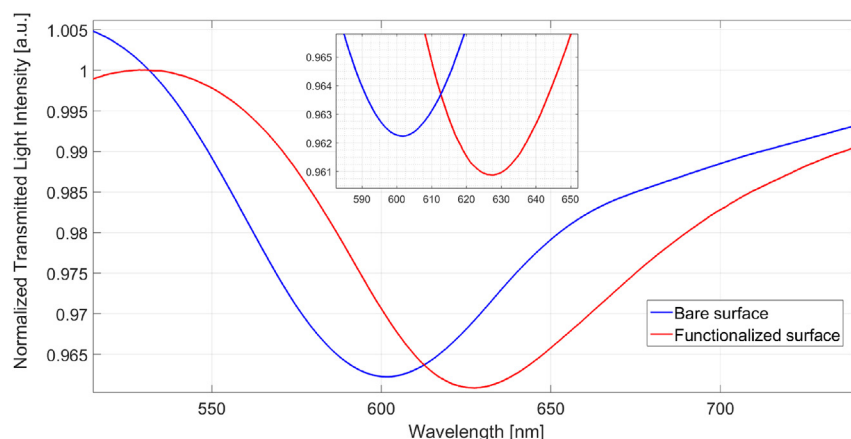


**Figure 1. Plasmonic spectra relative to the functionalization of the proposed SPR-POF chip**

The sensing surface was functionalized by exploiting the chemistry of lipoic acid/EDC/NHS for the cross-linking of the anti-IL-1 $\beta$  antibody (see STAR Methods for details). The passivation of unbound carboxyl groups was performed with ethanolamine and, finally, the plasmonic spectrum was acquired (red curve) and compared to that registered for a non-functionalized SPR-POF (blue curve). The inset highlights the magnification of the picks.

The aim of this study is to exploit SPR phenomena to develop a novel, highly sensitive, easily portable IL-1 $\beta$  point-of-care biosensor. SPR and Localized SPR (LSPR) are extensively used as label-free detection principles to realize sensitive biosensors operating in different applications. When a receptor layer is combined with the plasmonic surface to obtain the specificity for the biochemical detection of substances, the receptor selectively recognizes and captures the analyte present in a liquid sample. This produces a refractive index variation in contact with the metal surface, causing a change in the plasmonic phenomena. The extent of the refractive index variation depends on the analyte molecule structure, the receptor layer's efficiency, and the plasmonic sensitivity.<sup>60</sup>

SPR biosensors based on Kretschmann and Otto configurations are usually bulky and require expensive optical components. These configurations are difficult to miniaturize and cannot be used outside the laboratory scenario. The use of optical fibers improves plasmonic performances, allows remote sensing, and may reduce the device's cost and dimensions. In particular, to realize SPR platforms, plastic optical fibers (POFs) are especially advantageous due to their excellent flexibility, easy manipulation, great numerical aperture, large diameter, and the fact that plastic can withstand smaller bend radii than silica. Therefore, POF-based SPR sensors are simpler to realize and present several advantages than those based on silica optical fibers.<sup>61</sup> Recently, several SPR-based point-of-care tests (POCTs) use multimode POFs, associated with simple setups and different recognition elements, to realize agile sensor systems useful for detecting several types of analytes.<sup>60–66</sup> Plasmonic POCTs based on nanostructures or nanoparticles combined with specific receptors have been published recently.<sup>67</sup> The use of

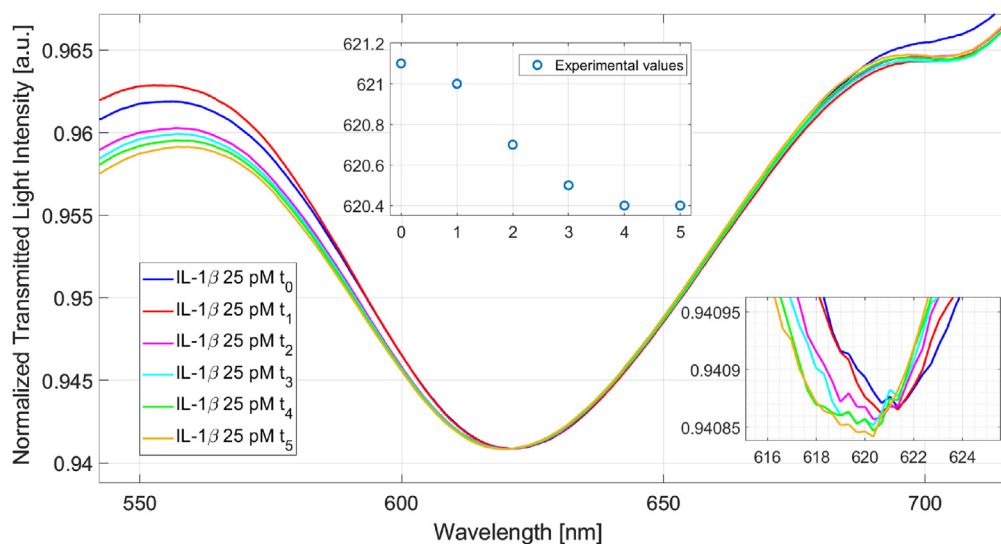


**Figure 2. Selection of the incubation time for IL-1 $\beta$  SPR-POF-biosensor response in buffer solution**

The times in the legend ( $t_0$ - $t_5$ ) represent the minutes (from 0 to 5) of the SAM exposure to the IL-1 $\beta$  solution (25 pM). On the right, the inset highlights the magnification of the picks. The inset in the upper part shows the registered resonance wavelengths plotted vs. the selected incubation times.

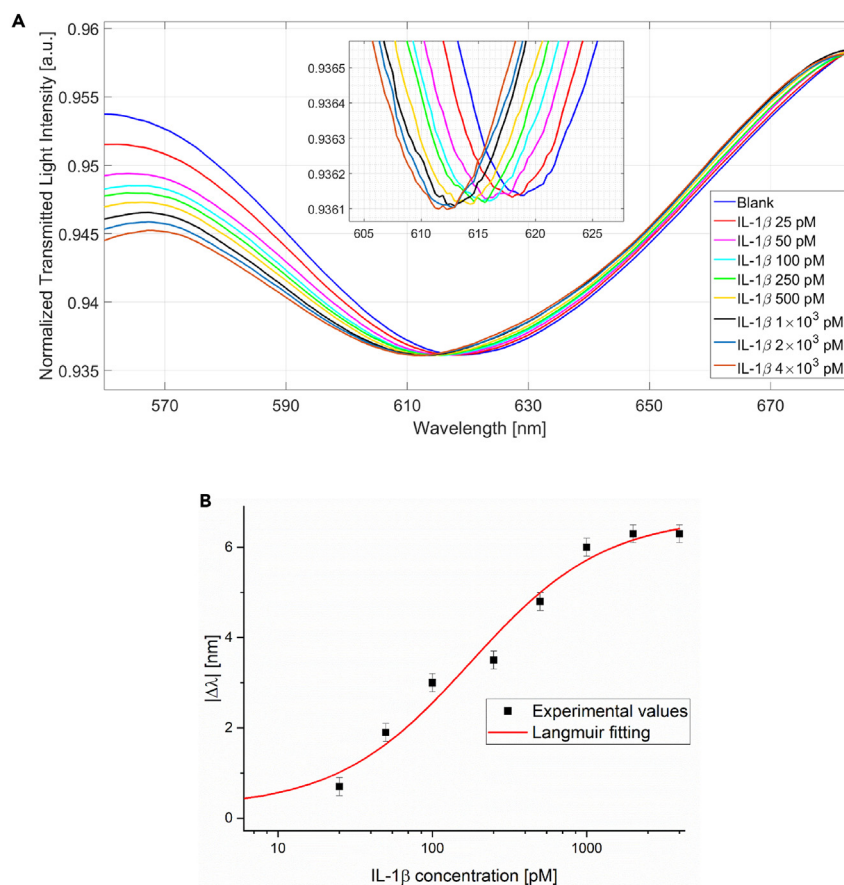


**Figure 3. IL-1 $\beta$  SPR-POF biosensor response in buffer solution**

(A) SPR spectra at different IL-1 $\beta$  concentrations ranging from 25 to  $4 \times 10^3$  pM. The solutions were prepared as sequential dilutions starting from the most concentrated and analyzed from the lowest to the highest concentration.

(B) Dose-response curve and Langmuir fitting of the collected data. Values are the mean of measurements performed in triplicates and error bars correspond to the major value of the standard deviations.

highly specific antibodies represents the most straightforward choice for biosensor molecular recognition, and technological progresses are constantly made for obtaining sensitive, reliable, and quantitative determinations.<sup>68</sup>

The presented SPR-POF chip adopts a highly sensitive and specific anti-IL1 $\beta$  antibody self-assembled monolayer (SAM) as sensing surface and exhibits a LoD in the picomolar range as well as very short times of analysis. This allows IL-1 $\beta$  monitoring in buffer solution and, importantly, in a complex biological matrix like saliva. As a proof of concept, we tested our biosensor on saliva samples from healthy and periodontitis subjects and validated the obtained measurements of salivary IL-1 $\beta$  through automated ELISA. The performances of the proposed technology will make our POCT a valuable tool for detecting IL-1 $\beta$  at the patient's side as a key marker for a timely diagnosis of oral inflammatory diseases, enabling an early, effective, and personalized treatment.

## RESULTS

### Production and characterization of the SAM specific for IL-1 $\beta$

To develop a sensitive SPR-POF for IL-1 $\beta$  detection, a plasmonic surface manufactured as in<sup>62</sup> was functionalized with an anti-human IL-1 $\beta$  antibody, as described in detail in the STAR Methods. First, to evaluate the efficiency of the functionalization process, the plasmonic spectra obtained by dropping on the sensitive surface double distilled (Milli-Q) water before and after each step of the functionalization procedure (including incubation with lipoic acid, NHS/EDC, IL-1 $\beta$  antibody, and ethanolamine buffer) were recorded. Particularly, as shown in Figure 1, it was evident the shift of about +25 nm of the resonance wavelength caused by the whole functionalization process, with the IL-1 $\beta$  antibody SAM (red curve) compared to that of the bare surface prior functionalization (blue curve). Indeed, as we previously reported,<sup>64–66</sup> this process results in a resonance wavelength shift to the right that typically ranges from 5 to 30 nm for an SPR-POF chip, due to an increase in the measured refractive index (RI) determined by the antibody SAM at the gold-dielectric interface in the presence of the same bulk refractive index (with the same bulk solution). If the change in RI is positive, the resonance wavelength increases, as in this case.

**Table 1. Langmuir parameters of the data fitting relative to IL-1 $\beta$  detection in buffer**

$\lambda_0$ [nm]		$\Delta\lambda_{\max}$ [nm]		K [pM]		Statistics	
Value	St. Error	Value	St. Error	Value	St. Error	$\chi^2$	R <sup>2</sup>
0.21515	0.49474	6.68541	0.31851	69.8783	28.1041	3.42071	0.97641

$\lambda_0$ , resonance wavelength measured in PBS without analyte;  $\Delta\lambda_{\max}$ , maximum value of  $\Delta\lambda$  calculated as the difference between the  $\lambda$  value at the saturation and the blank ( $\lambda_0$ ); K, fitting constant. Both the Langmuir and the statistical parameters ( $\chi^2$  and R<sup>2</sup>) of the fitting curve were calculated using the OriginPro software.

For a characterization of the SAM, the sensing surface of the chip was exactly reproduced by stratification and functionalization on cover glasses and experiments of immunofluorescence were performed as described under “STAR Methods” section. As shown in Figure 1 of the Supplementary Materials (Figure S1), a strong fluorescent signal could evidence the anti-IL-1 $\beta$  primary antibodies correctly linked on the surface, while no signal was detectable on the glass area not incubated with the antibody during the proper functionalization step.

### SPR-POF IL-1 $\beta$ biosensor: Experimental tests in buffer solution

To determine whether the proposed SPR-POF chip was able to specifically detect IL-1 $\beta$  at concentrations suitable for clinical applications, a dose-response curve in PBS was obtained. In brief, sequential dilutions of human recombinant IL-1 $\beta$  protein (in its cleaved form) were prepared in PBS, starting from  $4 \times 10^3$  pM to 25 pM, a concentration lower than the IL-1 $\beta$  value reported for healthy saliva.<sup>49</sup> Thus, we chose a concentration range that largely includes physiological and pathological levels of the analyte. First, the incubation time, determined as the minimum time sufficient for the binding of recombinant IL-1 $\beta$  to the antibody, was experimentally assessed by using a fixed analyte concentration (25 pM) and acquiring plasmonic spectra at different incubation time points. It must be noted that, differently from the spectra relative to the functionalization of the proposed SPR-POF chip, when the analyte-receptor binding occurs, the refractive index of the receptor layer decreases, and thus the resonance wavelength decreases (shift on the left). This behavior is in accord with previous studies.<sup>63–66</sup> From the time-response curve reported in Figure 2, 3 min incubation was selected for all the measurements performed in buffered solutions.

Once the exposure time was defined, we focused on the dose-response curve. Figure 3A shows the spectra recorded at different IL-1 $\beta$  concentrations in PBS solution, after normalization to a reference spectrum obtained in air. More precisely, the tested IL-1 $\beta$  concentrations range from 25 pM to  $4 \times 10^3$  pM (blue curve for PBS only; from red to mustard-colored curves,  $25\text{--}4 \times 10^3$  pM of IL-1 $\beta$  concentration range). The analysis of the obtained spectra revealed that a progressive shift of the respective resonance wavelengths toward the left was registered with increasing IL-1 $\beta$  concentrations, indicating that IL-1 $\beta$  specific binding to the antibodies in the SAM determined a decrease in the refractive index. This behavior is similar to that previously observed for the detection of other analytes by SPR-POFs functionalized with their relative antibody SAM.<sup>64–66</sup>

Moreover, Figure 3B reports the dose-response curve obtained by plotting the absolute values of the resonance wavelength variations  $|\Delta\lambda|$  versus the IL-1 $\beta$  concentration in PBS, whereas  $|\Delta\lambda| = |\lambda_c - \lambda_0|$  has been calculated as the difference between the resonance wavelength at the specific analyte concentration ( $\lambda_c$ ) and that obtained in PBS without analyte ( $\lambda_0$ , blank). The reported values are the mean of three measurements and the error bars have been calculated as the major value of the standard deviations. A red Langmuir fitting curve could be obtained, with the relative equation (Equation 1).

$$|\Delta\lambda| = |\lambda_c - \lambda_0| = |\Delta\lambda_{\max}| \cdot \left( \frac{c}{K+c} \right) \quad (\text{Equation 1})$$

The parameters of the Langmuir fitting shown in Figure 3B (generated using the OriginPro software, Origin Lab. Corp, Northampton, MA, USA) are summarized in Table 1.

Starting from Equation 1, it was possible to calculate the sensitivity at low concentrations (Equation 2). Particularly, at low concentration where  $c \ll K$ , Langmuir Equation 1 is simplified to a linear relationship, and, at these very low concentrations, the slope of the Langmuir curve corresponds to the sensitivity (c). This allows to obtain another important parameter, i.e., the LoD (Equation 3), calculated as three times the standard deviation of the blank (Table 1) divided by the sensitivity at low concentration. Finally, the affinity constant ( $K_{\text{aff}}$ ) is the reciprocal value of the K parameter in the Langmuir equation (Equation 4).

$$\text{Sensitivity at low } c = \frac{\Delta\lambda_{\max}}{K} \quad (\text{Equation 2})$$

**Table 2. SPR-POF Biosensor parameters for IL-1 $\beta$  detection in buffer solution**

Sensor	Parameters	Value
IL-1 $\beta$ SPR-POF Biosensor	$K_{\text{aff}}$ [pM <sup>-1</sup> ]	0.014
	Sensitivity at low c [nm/pM]	0.096
	LoD [pM]	15.5

$K_{\text{aff}}$ , Affinity constant; LoD, Limit of Detection. OriginPro software was used for calculations.

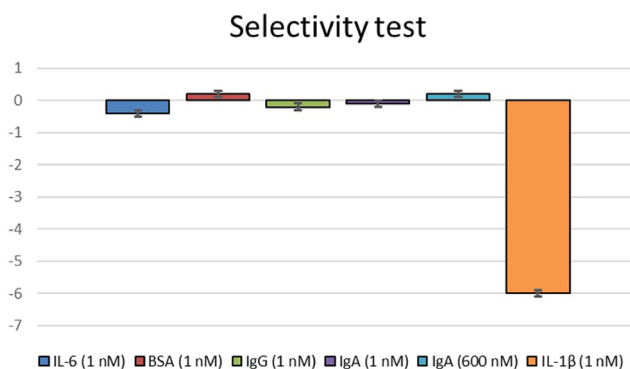


**Figure 4. IL-1β POF-Biosensor specificity test**

Resonance wavelength variation obtained for different recombinant proteins diluted in PBS at the reported concentrations. Interleukin 6 (IL-6), Bovine serum albumin (BSA), Immunoglobulin G (IgG), Immunoglobulin A (IgA), and IL-1β were analyzed. The wavelength variations ( $\Delta\lambda$ ) were calculated with respect to the blank (buffer only). Three measurements were performed for each determination and data are reported as mean value. The bars indicate standard deviations.

$$\text{LoD} = \frac{3 * \text{standard deviation of blank } (\lambda_0)}{\text{Sensitivity at low c}} \quad (\text{Equation 3})$$

$$K_{\text{aff}} = \frac{1}{K} \quad (\text{Equation 4})$$

Accordingly,  $K_{\text{aff}}$ , sensitivity at low c, and LoD were calculated for the proposed SPR-POF biosensor and the obtained results are reported in Table 2. Precisely, a LoD of 15.5 pM was reached.

Since low LoD and high selectivity are two critical parameters in developing a reliable method for the detection of a clinical biomarker in real matrices, the specificity of the proposed IL-1β detection system was tested by evaluating its response to recombinant BSA (1 nM) and the proinflammatory cytokine IL-6 (1 nM). IgG (1 nM) and IgA (1 nM and 600 nM) were also tested since both found in saliva as important humoral component of the salivary immunity.<sup>69</sup> It must be noted that the normal concentration of IgA in saliva is about 10 mg/dL, 300 nM. Upon incubation, the resonance spectra were recorded, and the plasmonic  $\Delta\lambda$  were calculated for each biomolecule, as detailed above. As shown in the histogram chart reported in Figure 4, all the analyzed proteins determined a negligible wavelength variation compared to the relevant negative shift of about 6 nm caused by IL-1β 1 nM, suggesting a very high specificity of the system in detecting IL-1β.

A further important property of any sensing system is its stability. The proposed SPR platforms, when not functionalized, can be left dried for a prolonged period of time (about 6 months). After the functionalization process, the biosensors can be normally stored in solution, particularly in PBS, pH 7.4 or in the specific Ab storing buffer (without glycerol), at 4°C. Thus, we evaluated the stability to low pH and durability of our chip. Three SPR surfaces were contemporaneously and equally functionalized with anti-IL-1β antibodies. 25 pM IL-1β solution was used for all the subsequent measures. 5 min of incubation with 100 mM Glycine-HCl, pH 2.2, were used to test the stability at low pH and as a potential regeneration strategy of the sensing SAM. It must be underlined that Glycine-HCl buffer is amply used to break the Ag-Ab interaction (in particular, to separate antigens from antibodies covalently bound to a matrix) and, thus, to regenerate immunospecific matrices.

Following, the description of the chips and the performed treatments and measurements, also schematized in the "Supplementary Materials" (Figure S2) is reported:

Chip#1: read at  $t_0$  (chip#1  $t_0$ ), immediately regenerated and reused for measurements (chip#1-R);

Chip#2: read at  $t_0$  (chip#2  $t_0$ ), immediately regenerated, stored in Ab storage buffer, and used for spectra acquisition after 6 weeks (chip#2-R  $t_{6w}$ );

Chip#3: stored directly after functionalization and used for the analysis after 6 weeks (chip#3  $t_{6w}$ ), then regenerated and reused for spectra acquisition (chip#3  $t_{6w}$ -R).

The measured  $\Delta\lambda$  did not show significant variations compared to  $\Delta\lambda$  of their proper controls (Figure S2) suggesting the stability of the biosensor over time and after a low pH treatment.

### SPR-POF IL-1β biosensor: Experimental test in saliva

Based on the obtained results, the proposed SPR-POF biosensor was tested to detect IL-1β in a highly complex real-life matrix like saliva. More in detail, human saliva from a healthy volunteer was diluted 1:50 in PBS to prepare serial dilutions of IL-1β, as those made in PBS. These solutions were then analyzed for obtaining the relative SPR spectra, shown in Figure 5A, to be used for the construction of the IL-1β dose-response curve in saliva. Figure 5B shows the mean values of the experimental determinations obtained in triplicate, with the relative error bars and the Langmuir fitting curve.

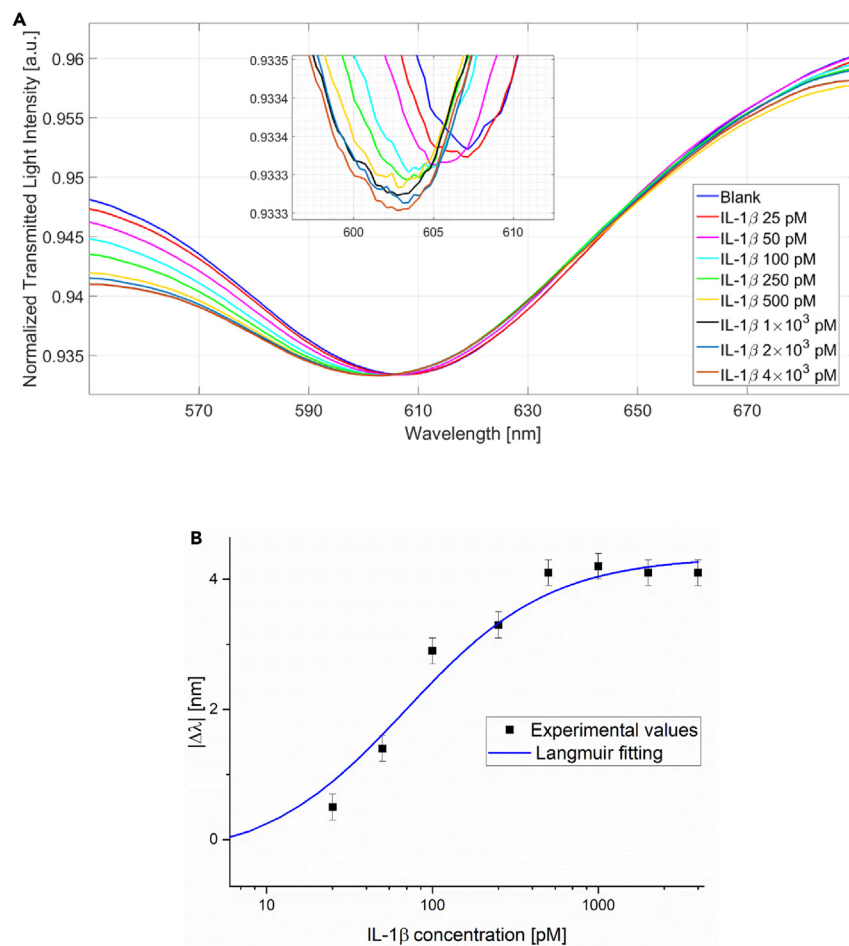


**Figure 5. Dose-response curve for the measurements of IL-1β in human saliva**

(A) SPR spectra obtained at different concentrations, starting from the blank (diluted healthy human saliva without any addition) to  $4 \times 10^3$  pM recombinant IL-1β diluted in saliva. The inset highlights the magnification of the curve picks.

(B)  $\Delta\lambda$  is calculated with respect to the blank. Measurements at different concentration of IL-1β in human saliva (diluted 1:50) were performed in triplicates and the obtained mean values are reported. The error bars correspond to the major value of the standard deviations. The blue curve represents the Langmuir fitting of the experimental values.

The obtained Langmuir parameters are reported in Table 3. The calculated  $K_{aff}$ , sensitivity at low concentrations, and LoD of the biosensor in diluted saliva are reported in Table 4. Thus, the proposed biosensor showed high sensitivity in saliva and a LoD of 23.4 pM. Since the LoD and sensitivity in saliva are mainly in the same order of magnitude as in PBS, it can be assumed that the detection is scarcely affected by the high complexity of the matrix and, therefore, the system may be suitable and reliable for the determination of the low concentration of IL-1β also in other complex biological fluids, like the serum.

From both calibration curves (in buffer solution and in real matrix), dynamic linear ranges (in buffer solution and saliva tests) (Figure 6) and the relative equations (Equations 5 and 6) were calculated by using OriginPro software. Wide linear dynamic concentration ranges were obtained over which a linearly changing instrumental response is observed (25–1000 pM for test in buffer solution, and, importantly, 25–500 pM for tests in saliva). The derived mathematical function allows direct calculation of IL-1β concentrations in the reported ranges of both physiological and pathological conditions.

$$\Delta\lambda_{out} = (0.005 \pm 0.001) \cdot c + (1.82 \pm 0.48) \quad (\text{Equation 5})$$

$$\Delta\lambda_{out} = (0.006 \pm 0.002) \cdot c + (1.25 \pm 0.55) \quad (\text{Equation 6})$$

$\Delta\lambda_{out}$  corresponds to the difference between the output wavelength of the sample and that of blank, and  $c$  indicates the IL-1β concentration (pM). The related statistical parameters, i.e., Pearson correlation coefficient and  $R^2$ , for the strength of the linear relationship between  $\Delta\lambda_{out}$  and  $c$  are equal to 0.91 and 0.8 for (5), 0.86, and 0.66 for (6), respectively.



**Table 3. Langmuir parameters of the fitting relative to IL-1 $\beta$  detection in diluted saliva**

Matrix	$\lambda_0$ [nm]		$\Delta\lambda_{\max}$ [nm]		K [nM]		Statistics	
	Value	St. Error	Value	St. Error	Value	St. Error	$\chi^2$	R <sup>2</sup>
Diluted Saliva (1:50)	-0.35171	0.49182	4.34678	0.23396	69.4223	39.8834	0.12011	0.95699

$\lambda_0$ , resonance wavelength measured in PBS without analyte;  $\Delta\lambda_{\max}$ , maximum value of  $\Delta\lambda$  calculated as the difference between the  $\lambda$  value at the saturation and the blank ( $\lambda_0$ ); K, fitting constant. Both the Langmuir and the statistical parameters ( $\chi^2$  and R<sup>2</sup>) of the fitting curve for IL-1 $\beta$  detection in human saliva (diluted 1:50) were calculated using the OriginPro software.

A direct correlation between wavelength variations observed in PBS and in saliva for IL-1 $\beta$  measurement (plot shown in Figure S3) allows the calculation of a correlation coefficient of 0.94446423.

### Monitoring of salivary IL-1 $\beta$ levels related to periodontal healthy and pathological conditions

As a proof-of-concept, to preliminary evaluate the real applicability of the IL-1 $\beta$  dosage by the developed POCT in the diagnosis and monitoring of periodontitis, a pilot experiment was carried out to measure IL-1 $\beta$  concentration in saliva samples collected from a periodontally healthy subject (control) and from a periodontitis patient. The criteria adopted for the selection of the two donors are described in the STAR methods, “experimental model and study participant details” Section. Both samples were diluted 1:2 in PBS and analyzed by the proposed IL-1 $\beta$ -SPR-POF. As shown in Figure 7A, when the healthy sample was incubated on the sensing surface, the resonance wavelength shifted approximately 0.7 nm toward the left (red curve) compared to the blank (blue curve). This shift corresponds to an IL-1 $\beta$  concentration of about 40 pM, as obtained from the Langmuir fitting (reported in Figure 5B) of  $\Delta\lambda$  obtained in saliva (Figure 5A) and from the linear curve (blue) reported in Figure 6.

Furthermore, when the saliva from the periodontitis patient was incubated on the sensing surface, a shift of the red curve toward the left of about 2.5 nm was observed (Figure 7B). Accordingly, the IL-1 $\beta$  concentration in the patient saliva, determined by interpolation on the orange straight curve in Figure 6 and considering the sample dilution, was estimated to be 210 pM.

Simultaneously, the diluted samples were also analyzed through an automated ELISA as reported in the STAR Methods section. The test, based on the contemporaneous determination of multiple analytes in multiple samples on cartridges, requires about 2 h for results, as well as a quite expensive and bulky reader apparatus and plates; so, despite being this strategy a very sensitive hands-off technology, it cannot be considered a point-of-care system; nevertheless, it is the gold standard for precise determination of the analyte concentrations. Considering the dilution of samples, the concentration of IL-1 $\beta$ , obtained from the calibration curve of the commercial immunoassay (log blue curve in Figure 8), were 45 pM (764 pg/mL; %CV = 0.98) and 200 pM (3,351 pg/mL; %CV = 7.96) in healthy and patient saliva specimens (yellow points on the curve, Figure 8), respectively. The finding appears of great importance in validating the IL-1 $\beta$  measurements obtained by our developed POF.

To test background noise of saliva components, we compare the concentration values of IL-1 $\beta$  in the analyzed patient saliva estimated from both the dose-response curves (that built in PBS and that obtained using saliva diluted 1:50) with close results (201 pM and 210 pM, respectively) (Figure S4). It is important to state that ELISA determination of IL-1 $\beta$  in the same sample gave a 200 p.m. concentration value. Furthermore, a second pathological saliva specimen (sample 2) diluted 1:10 was analyzed through the SPR device and IL-1 $\beta$  concentrations were estimated from the two dose-response curves as above. Again, the concentrations determined were comparable (250 pM and 259 pM, respectively), confirming the not relevant interference of matrix components (Figure S4).

Based on the obtained results, our SPR-POF POCT appears highly sensitive and specific for the real-time monitoring of IL-1 $\beta$  in saliva and effective in recognizing the interleukin at both low (physiological) and high (pathological) concentrations after only 3 min of incubation time. Thus, it can provide a valuable help for the diagnosis and the management of periodontitis at the chair-side.

## DISCUSSION

The potential for using salivary biomarkers as indicators of systemic and/or oral health status has been emphasized by recent investigations<sup>34,70,71</sup> and by the National Institutes of Health recommendation, so that saliva might be considered a valuable analytical biofluid, replicating, in many cases, the blood.<sup>72</sup>

Focusing on oral health, inflammation and degradation of connective tissue, along with periodontium bone remodeling, can be specifically associated with a number of potential biomarkers.<sup>73,74</sup> A general definition of “biomarker” is “a characteristic that is measured as an indicator of normal biological processes, pathogenic processes, or a response to an exposure or intervention” (FDA-NIH Biomarker Working

**Table 4. Biosensor parameters for IL-1 $\beta$  detection in diluted saliva**

Sensor	Parameters	Value
IL-1 $\beta$ SPR-POF	K <sub>aff</sub> [pM <sup>-1</sup> ]	0.014
Biosensor	Sensitivity at low c [nm/pM]	0.063
	LoD [pM]	23.4

K<sub>aff</sub>, Affinity constant; LoD, Limit of Detection. OriginPro software was used for calculations.

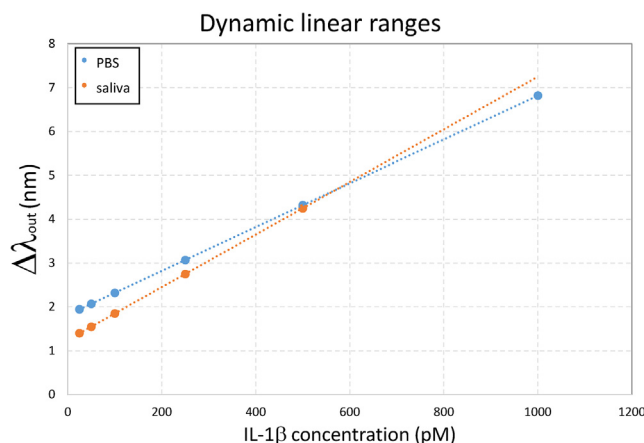


**Figure 6. Evaluation of dynamic linear ranges for measurements in buffer (PBS, light blue) and real matrix (saliva, orange)**

$\Delta\lambda_{out}$  represents the difference between the output wavelength of the sample and the output wavelength of the blank, calculated for all the included IL-1 $\beta$  concentrations.

Group, 2016). Hence, the identification of a biomarker and the determination of its concentrations in biological fluids, such as saliva, have important clinical implications. Regarding periodontitis, inflammatory cytokines such as IL-1 $\beta$  and IL-6, MIP-1 $\alpha$ , and metalloproteinase such as MMP-8 (particularly in its active form) are, among the biomolecules released in GCF and saliva, the most promising to be referred to as biomarkers of the condition, often detectable even before the appearance of the radiographic and clinical signs of gingival and alveolar bone damage.<sup>49</sup> Particularly, IL-1 $\beta$  can be considered a very precocious biomarker of periodontium diseases, being secreted in response to the bacterial infections and strongly contributing to the host inflammatory response. Furthermore, IL-1 $\beta$ , in combination with MMP-8, is able to discriminate periodontal health from periodontitis in condition of concomitant systemic inflammatory-associated diseases such as type 2 diabetes mellitus.<sup>75</sup> Also, as demonstrated by a very recent meta-analysis, the accuracy of early periodontitis diagnosis can be strongly increased through detection of IL-1 $\beta$  in combination with other biomarkers in saliva.<sup>76</sup> In particular, combination of IL-1 $\beta$  with MMP-8, or with IL-6, and IL-6 with MMP-8 measurements would allow correct identification of 78%–81% of periodontitis patients and the exclusion of

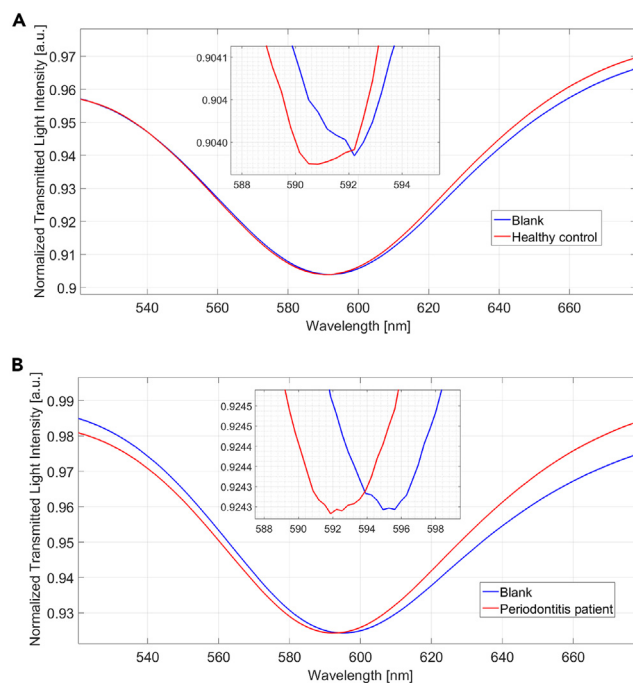


**Figure 7. Determination of IL-1 $\beta$  levels in periodontal healthy and pathological saliva**

SPR spectra were obtained by the developed biosensor probing saliva samples from a healthy (A) and a periodontitis patient (B). The saliva samples were diluted 1:2 in PBS. The SAMs were exposed to each sample for 3 min only.

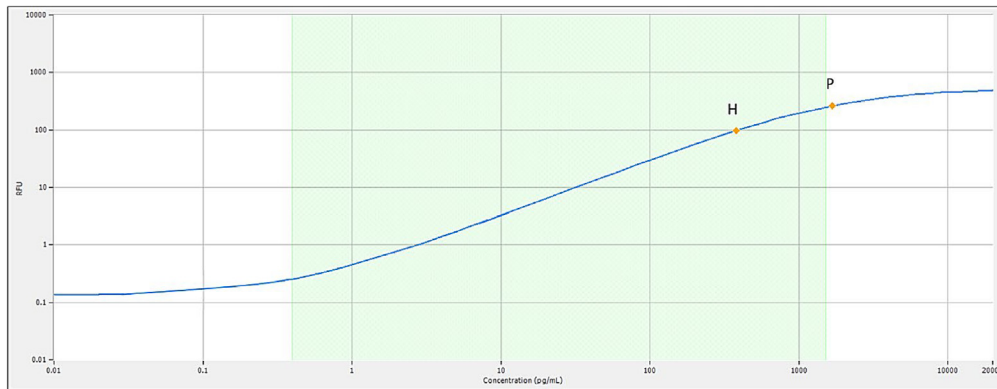


**Figure 8. Graphical representation of IL-1 $\beta$  concentration (pg/mL) obtained by automated ELISA immunoassay**

The healthy (H) and the periodontitis patient (P) saliva samples were analyzed by using the ELLA system (ProteinSimple, San Jose, CA, USA) after a 1:2 dilution in the ELLA dilution buffer. Each measure was performed in duplicate. Blue curve: standard curve. Green range: dynamic range of the assay.

85–88% of non-periodontitis subjects. Unfortunately, the level of salivary components is rarely determined in oral and systemic clinical practice. The scarcity of definite data is mainly due to the variability of component concentration, strictly depending on the saliva sampling method.<sup>48</sup> In addition, the analytical assessment of levels of biomarkers such as those of cytokines, mainly by ELISA methods, entails high costs and time for results. In this scenario, portable devices favoring the analyses at the patient point-of-care represent an important diagnostic advancement. So, intensive multidisciplinary efforts have focused on developing highly performant POCT. However, only a small number of these medical devices are today available for accurate measurements on saliva.

The proposed IL-1 $\beta$  SPR-POF POCT respects all the WHO criteria (2006) defined for point-of-care technologies and represents a promising tool for an early diagnosis of periodontitis (prior to the evidence of tissue damage) and for monitoring the disease evolution and the effectiveness of therapeutic interventions.<sup>77–79</sup> Importantly, the IL-1 $\beta$  measurements obtained on the saliva samples from a healthy and a periodontitis patient were superimposable with those obtained by ELISA (the gold standard for cytokine determination). This finding contributes to validating the developed biosensor for precise detection of IL-1 $\beta$ .

Furthermore, the device has been designed to be implemented for the dosage of the other markers, i.e., IL-6,<sup>66</sup> MMP-8,<sup>64</sup> MIP-1 $\alpha$ ,<sup>80</sup> and malondialdehyde as oxidative stress marker,<sup>65</sup> whose salivary levels have been associated with the pathology. Recent investigations also propose IL-1 $\beta$  detection, with IL-6 and other proinflammatory cytokines, in COVID-19 patients as early biomarker for predicting progression to severe illness and negative prognosis, and in following disease progression in long COVID.<sup>81</sup> Accordingly, intensive efforts are dedicated to detect such cytokines in non-invasive bodily fluid as saliva. Thus, our biosensor and its upgraded set-ups could represent an intriguing and feasible method for real-time cytokine monitoring in these clinical settings.

The good performance in the highly complex system of saliva (not interfering with our measurements) implies the potential application of the developed chip to other liquid biospecimens (for clinical applications) and cell culture media (for scientific research). Finally, since IL-1 $\beta$  has been proposed as a biomarker for numerous pathologies, including peri-implant diseases,<sup>21</sup> allergic rhinitis,<sup>14</sup> rheumatoid arthritis,<sup>13</sup> and not least cancer,<sup>15–17</sup> our device might greatly expand its applicability.

Regarding future commercialization perspective, the proposed sensing approach is very low-cost with respect to other SPR-based sensors. In particular, the cost of the equipment to implement the setup (the spectrometer and the white light source) is about 5 k euros, whereas the cost per SPR-POF probe is less than 10 euros. The functionalization process cost is a function of the used receptor. In particular, in order to obtain the sensor's reproducibility on an industrial scale, molecularly imprinted polymers (MIPs) can be used instead of bio-receptor layers. More specifically, the sensor price is around a few euros per chip when MIPs are used. In fact, this biomimetic receptor presents several favorable aspects in comparison to other bioreceptors (aptamers, antibodies, etc.), including better stability out of the native environment, use in complex matrices, versatility by the changing of the imprinting, low cost, and reproducibility on an industrial scale.

### Limitations of the study

Despite the proposed technology can be used for tests at the point of patient care, some improvements can be made to render it more affordable. First, its large-scale production will certainly require further cost cuts, which could be achieved through antibody self-manufacturing or, alternatively and more cheaply, by applying different sensing surfaces with a predetermined selectivity against the secreted form of IL-1 $\beta$ . Furthermore, due to the identification of *IL1B* mutations, surfaces specifically designed for the variants might be made more selective and, then, overcome potential low-affinity surfaces due to changes of the 3D structure of the mutated cytokine. Importantly, although IL-1 $\beta$  is a promising biomarker of periodontitis, its detection alone may not allow for a definite diagnosis due to the broad spectrum of diseases causing its elevation in human saliva. We are currently working on implementing our technology for a multiplexed assay that will allow for the simultaneous detection and measurement of different biomarkers, strongly increasing the sensitivity and specificity of the diagnostic method and resulting in a definite diagnosis, tailored therapy, precise monitoring of disease progression, and response to treatments. Finally, due to the

IL-1 $\beta$  lower levels in other biological fluids like plasma (both in pathological and physiological conditions), we are working toward changing the ranges and reducing the limit of detection by using extrinsic polymer-based nanoplasmonic chip as performed in Cennamo et al., 2023<sup>66</sup>; this kind of technology will provide an important step forward for detecting and monitoring some inflammation-based systemic diseases.

## STAR★METHODS

Detailed methods are provided in the online version of this paper and include the following:

- KEY RESOURCES TABLE
- RESOURCE AVAILABILITY
  - Lead contact
  - Materials availability
  - Data and code availability
- EXPERIMENTAL MODEL AND STUDY PARTICIPANT DETAILS
  - Patient samples
- METHOD DETAILS
  - Chemicals and reagents
  - SPR optical fiber sensor system
  - Functionalization of SPR-POF plasmon surfaces and immunofluorescence
  - IL-1 $\beta$  binding test in buffer solution and saliva and specificity and stability test
  - Determination of salivary IL-1 $\beta$  concentration in periodontitis saliva
- QUANTIFICATION AND STATISTICAL ANALYSIS

## SUPPLEMENTAL INFORMATION

Supplemental information can be found online at <https://doi.org/10.1016/j.isci.2023.108741>.

## ACKNOWLEDGMENTS

The authors acknowledge the VALERE Program of the University of Campania “Luigi Vanvitelli” (to F.D.R. and N.C.), BETTER Project, funded by Regione Campania - POR FESR CAMPANIA 2014-2020 - OS 1.3 - Azione 1.3.1 (to L.Z. and N.C.), AIM Attrazione e Mobilità Internazionale del MIUR (for E.S. salary), Programma VALERE: Vanvitelli per la Ricerca (for D.B. salary), and Bando di Ateneo (Vanvitelli) per il finanziamento di progetti di ricerca fondamentale ed applicata dedicato ai giovani Ricercatori: Kip2PTMcaTR (CUP:B63C22001470005 to E.S.).

## AUTHOR CONTRIBUTIONS

Conceptualization: N.C., D.B., M.A., F.D.R., L.Z., L.G., and A.B. Methodology: N.C., D.B., L.Z., L.G., and A.B. Investigation: N.C., D.B., M.A., F.A., E.S., and A.P. Data curation & formal analysis: N.C., D.B., M.A., F.A., L.Z., and A.B. Validation: N.C., D.B., M.A., F.A., L.Z., L.G., and A.B. Supervision: N.C., L.Z., L.G., and A.B. Writing – original draft: N.C., D.B., M.A., F.A., E.S., A.P., F.D.R., L.Z., L.G., and A.B. Writing – review and editing: N.C., D.B., M.A., F.D.R., L.Z., L.G., and A.B.

## DECLARATION OF INTERESTS

The authors declare no competing interests.

Received: July 5, 2023

Revised: November 17, 2023

Accepted: December 12, 2023

Published: December 14, 2023

## REFERENCES

1. Palomo, J., Dietrich, D., Martin, P., Palmer, G., and Gabay, C. (2015). The interleukin (IL)-1 cytokine family—Balance between agonists and antagonists in inflammatory diseases. *Cytokine* 76, 25–37.
2. Kaneko, N., Kurata, M., Yamamoto, T., Morikawa, S., and Masumoto, J. (2019). The role of interleukin-1 in general pathology. *Inflamm. Regen.* 39, 12.
3. Dinarello, C.A. (2002). The IL-1 family and inflammatory diseases. *Clin. Exp. Rheumatol.* 20, S1–S13.
4. Dinarello, C.A. (2018). Overview of the IL-1 family in innate inflammation and acquired immunity. *Immunol. Rev.* 281, 8–27.
5. Liu, Y.C.G., Lerner, U.H., and Teng, Y.T.A. (2010). Cytokine responses against periodontal infection: protective and destructive roles. *Periodontol.* 2000 52, 163–206.
6. Kwak, A., Lee, Y., Kim, H., and Kim, S. (2016). Intracellular interleukin (IL)-1 family cytokine processing enzyme. *Arch. Pharm. Res.* 39, 1556–1564.
7. Franchi, L., Muñoz-Planillo, R., and Núñez, G. (2012). Sensing and reacting to microbes through the inflammasomes. *Nat. Immunol.* 13, 325–332.
8. Panagakos, F.S., Jandinski, J.J., Feder, L., and Kumar, S. (1994). Effects of plasminogen and interleukin-1 beta on bone resorption in vitro. *Biochimie* 76, 394–397.
9. Jimi, E., Nakamura, I., Duong, L.T., Ikebe, T., Takahashi, N., Rodan, G.A., and Suda, T. (1999). Interleukin 1 induces multinucleation and bone-resorbing activity of osteoclasts in

- the absence of osteoblasts/stromal cells. *Exp. Cell Res.* 247, 84–93.
10. Lee, Y.M., Fujikado, N., Manaka, H., Yasuda, H., and Iwakura, Y. (2010). IL-1 plays an important role in the bone metabolism under physiological conditions. *Int. Immunol.* 22, 805–816.
  11. Niki, Y., Yamada, H., Seki, S., Kikuchi, T., Takaishi, H., Toyama, Y., Fujikawa, K., and Tada, N. (2001). Macrophage- and neutrophil-dominant arthritis in human IL-1 alpha transgenic mice. *J. Clin. Invest.* 107, 1127–1135.
  12. Polzer, K., Joosten, L., Gasser, J., Distler, J.H., Ruiz, G., Baum, W., Redlich, K., Bobacz, K., Smolen, J.S., van den Berg, W., et al. (2010). Interleukin-1 is essential for systemic inflammatory bone loss. *Ann. Rheum. Dis.* 69, 284–290.
  13. Dissanayake, K., Jayasinghe, C., Wanigasekara, P., and Sominanda, A. (2021). Potential applicability of cytokines as biomarkers of disease activity in rheumatoid arthritis: Enzyme-linked immunosorbent spot assay-based evaluation of TNF- $\alpha$ , IL-1 $\beta$ , IL-10 and IL-17A. *PLoS One* 16, e0246111.
  14. Han, M.W., Kim, S.H., Oh, I., Kim, Y.H., and Lee, J. (2021). Obesity Can Contribute to Severe Persistent Allergic Rhinitis in Children through Leptin and Interleukin-1 $\beta$ . *Int. Arch. Allergy Immunol.* 182, 546–552.
  15. Idris, A., Ghazali, N.B., and Koh, D. (2015). Interleukin 1 $\beta$ -A Potential Salivary Biomarker for Cancer Progression? *Biomark. Cancer* 7, 25–29.
  16. Garon, E.B., Chih-Hsin Yang, J., and Dubinett, S.M. (2020). The Role of Interleukin 1 $\beta$  in the Pathogenesis of Lung Cancer. *JTO Clin. Res. Rep.* 1, 100001.
  17. Maker, A.V., Katabi, N., Qin, L.X., Klimstra, D.S., Schattner, M., Brennan, M.F., Jarnagin, W.R., and Allen, P.J. (2011). Cyst fluid interleukin-1beta (IL1beta) levels predict the risk of carcinoma in intraductal papillary mucinous neoplasms of the pancreas. *Clin. Cancer Res.* 17, 1502–1508.
  18. Coussens, L.M., and Werb, Z. (2002). Inflammation and cancer. *Nature* 420, 860–867.
  19. Graves, D.T., and Cochran, D. (2003). The contribution of interleukin-1 and tumor necrosis factor to periodontal tissue destruction. *J. Periodontol.* 74, 391–401.
  20. Cheng, R., Wu, Z., Li, M., Shao, M., and Hu, T. (2020). Interleukin-1 $\beta$  is a potential therapeutic target for periodontitis: a narrative review. *Int. J. Oral Sci.* 12, 2.
  21. Gomes, A.M., Douglas-de-Oliveira, D.W., Ferreira, S.D., Silva, T.A.D., Cota, L.O.M., and Costa, F.O. (2019). Periodontal disease, peri-implant disease and levels of salivary biomarkers IL-1 $\beta$ , IL-10, RANK, OPG, MMP-2, TGF- $\beta$  and TNF- $\alpha$ : follow-up over 5 years. *J. Appl. Oral Sci.* 27, e20180316.
  22. Akiyama, T., Miyamoto, Y., Yoshimura, K., Yamada, A., Takami, M., Suzawa, T., Hoshino, M., Imamura, T., Akiyama, C., Yasuhara, R., et al. (2014). Porphyromonas gingivalis-derived lysine gingipain enhances osteoclast differentiation induced by tumor necrosis factor- $\alpha$  and interleukin-1 $\beta$  but suppresses that by interleukin-17A: importance of proteolytic degradation of osteoprotegerin by lysine gingipain. *J. Biol. Chem.* 289, 15621–15630.
  23. Papananou, P.N., Sanz, M., Buduneli, N., Dietrich, T., Feres, M., Fine, D.H., Flemmig, T.F., Garcia, R., Giannobile, W.V., Graziani, F., et al. (2018). Periodontitis: Consensus report of workgroup 2 of the 2017 World Workshop on the Classification of Periodontal and Peri-Implant Diseases and Conditions. *J. Periodontol.* 89, S173–S182.
  24. Kassebaum, N.J., Bernabé, E., Dahiya, M., Bhandari, B., Murray, C.J., and Marcenes, W. (2014). Global Burden of Severe Tooth Loss: A Systematic Review and Meta-analysis. *J. Dent. Res.* 93, 205–285.
  25. Cecero, G., Annunziata, M., Iuorio, M.T., Nastri, L., and Guida, L. (2020). Periodontitis, Low-Grade Inflammation and Systemic Health: A Scoping Review. *Medicina (Kaunas, Lithuania)* 56, 272.
  26. Martínez-García, M., and Hernández-Lemus, E. (2021). Periodontal Inflammation and Systemic Diseases: An Overview. *Front. Physiol.* 12, 709438.
  27. Sanz, M., and Kornman, K.; working group 3 of the joint EFP/AAP workshop (2013). Periodontitis and adverse pregnancy outcomes: consensus report of the Joint EFP/AAP Workshop on Periodontitis and Systemic Diseases. *J. Periodontol.* 84, S164–S169.
  28. Sanz, M., Ceriello, A., Buyschaert, M., Chapple, I., Demmer, R.T., Graziani, F., Herrera, D., Jepsen, S., Lione, L., Madianos, P., et al. (2018). Scientific evidence on the links between periodontal diseases and diabetes: Consensus report and guidelines of the joint workshop on periodontal diseases and diabetes by the International Diabetes Federation and the European Federation of Periodontology. *J. Clin. Periodontol.* 45, 138–149.
  29. Hansen, P.R., and Holmstrup, P. (2022). Cardiovascular Diseases and Periodontitis. *Adv. Exp. Med. Biol.* 1373, 261–280.
  30. Sanz, M., Marco Del Castillo, A., Jepsen, S., Gonzalez-Juanatey, J.R., D’Aiuto, F., Bouchard, P., Chapple, I., Dietrich, T., Gotsman, I., Graziani, F., et al. (2020). Periodontitis and cardiovascular diseases: Consensus report. *J. Clin. Periodontol.* 47, 268–288.
  31. Nwizu, N., Wactawski-Wende, J., and Genco, R.J. (2020). Periodontal disease and cancer: Epidemiologic studies and possible mechanisms. *Periodontology* 83, 213–233.
  32. Arias-Bujanda, N., Regueira-Iglesias, A., Balsa-Castro, C., Nibali, L., Donos, N., and Tomás, I. (2019). Accuracy of single molecular biomarkers in gingival crevicular fluid for the diagnosis of periodontitis: A systematic review and meta-analysis. *J. Clin. Periodontol.* 46, 1166–1182.
  33. Chen, M., Cai, W., Zhao, S., Shi, L., Chen, Y., Li, X., Sun, X., Mao, Y., He, B., Hou, Y., et al. (2019). Oxidative stress-related biomarkers in saliva and gingival crevicular fluid associated with chronic periodontitis: A systematic review and meta-analysis. *J. Clin. Periodontol.* 46, 608–622.
  34. Zhang, C.Z., Cheng, X.Q., Li, J.Y., Zhang, P., Yi, P., Xu, X., and Zhou, X.D. (2016). Saliva in the diagnosis of diseases. *Int. J. Oral Sci.* 8, 133–137.
  35. Miller, C.S., King, C.P., Jr., Langub, M.C., Kryscio, R.J., and Thomas, M.V. (2006). Salivary biomarkers of existing periodontal disease: a cross-sectional study. *J. Am. Dent. Assoc.* 137, 322–329.
  36. Christodoulides, N., Floriano, P.N., Miller, C.S., Ebersole, J.L., Mohanty, S., Dharshan, P., Griffin, M., Lennart, A., Ballard, K.L.M., King, C.P., Jr., et al. (2007). Lab-on-a-chip methods for point-of-care measurements of salivary biomarkers of periodontitis. *Ann. N. Y. Acad. Sci.* 1098, 411–428.
  37. Scannapieco, F.A., Ng, P., Hovey, K., Hausmann, E., Hutson, A., and Wactawski-Wende, J. (2007). Salivary biomarkers associated with alveolar bone loss. *Ann. N. Y. Acad. Sci.* 1098, 496–497.
  38. Sánchez, G.A., Miozza, V.A., Delgado, A., and Busch, L. (2013). Salivary IL-1 $\beta$  and PGE2 as biomarkers of periodontal status, before and after periodontal treatment. *J. Clin. Periodontol.* 40, 1112–1117.
  39. Frodge, B.D., Ebersole, J.L., Kryscio, R.J., Thomas, M.V., and Miller, C.S. (2008). Bone remodeling biomarkers of periodontal disease in saliva. *J. Periodontol.* 79, 1913–1919.
  40. Gomes, F.I.F., Aragão, M.G.B., Barbosa, F.C.B., Bezerra, M.M., de Paulo Teixeira Pinto, V., and Chaves, H.V. (2016). Inflammatory Cytokines Interleukin-1 $\beta$  and Tumour Necrosis Factor- $\alpha$  - Novel Biomarkers for the Detection of Periodontal Diseases: a Literature Review. *J. Oral Maxillofac. Res.* 7, e2.
  41. Stashenko, P., Dewhirst, F.E., Peros, W.J., Kent, R.L., and Ago, J.M. (1987). Synergistic interactions between interleukin 1, tumor necrosis factor, and lymphotoxin in bone resorption. *J. Immunol.* 138, 1464–1468.
  42. Masada, M.P., Persson, R., Kenney, J.S., Lee, S.W., Page, R.C., and Allison, A.C. (1990). Measurement of interleukin-1 alpha and -1 beta in gingival crevicular fluid: implications for the pathogenesis of periodontal disease. *J. Periodontol. Res.* 25, 156–163.
  43. Boch, J.A., Wara-aswapati, N., and Auron, P.E. (2001). Interleukin 1 signal transduction-current concepts and relevance to periodontitis. *J. Dent. Res.* 80, 400–407.
  44. Engebretson, S.P., Grbic, J.T., Singer, R., and Lamster, I.B. (2002). GCF IL-1beta profiles in periodontal disease. *J. Clin. Periodontol.* 29, 48–53.
  45. Ebersole, J.L., Schuster, J.L., Stevens, J., Dawson, D., 3rd, Kryscio, R.J., Lin, Y., Thomas, M.V., and Miller, C.S. (2013). Patterns of salivary analytes provide diagnostic capacity for distinguishing chronic adult periodontitis from health. *J. Clin. Immunol.* 33, 271–279.
  46. Ebersole, J.L., Nagarajan, R., Akers, D., and Miller, C.S. (2015). Targeted salivary biomarkers for discrimination of periodontal health and disease(s). *Front. Cell. Infect. Microbiol.* 5, 62.
  47. Kim, J.Y., Kim, K.R., and Kim, H.N. (2021). The Potential Impact of Salivary IL-1 on the Diagnosis of Periodontal Disease: A Pilot Study. *Healthcare (Basel, Switzerland)* 9, 729.
  48. Bellagambi, F.G., Lomonaco, T., Salvo, P., Vivaldi, F., Hanguët, M., Ghimenti, S., Biagini, D., Di Francesco, F., Fuoco, R., and Errachid, A. (2020). Saliva sampling: Methods and devices. An overview. *Trends Anal. Chem.* 124, 115781.
  49. Relvas, M., Silvestre, R., Gonçalves, M., Cabral, C., Mendes-Frias, A., Monteiro, L., and Viana da Costa, A. (2023). Analysis of Salivary Levels of IL-1 $\beta$ , IL17A, OPG and RANK-L in Periodontitis Using the 2017 Classification of Periodontal Diseases-An Exploratory Observational Study. *J. Clin. Med.* 12, 1003.
  50. Caton, J.G., Armitage, G., Berglundh, T., Chapple, I.L.C., Jepsen, S., Kornman, K.S., Mealey, B.L., Papananou, P.N., Sanz, M., and Tonetti, M.S. (2018). A new classification scheme for periodontal and peri-implant diseases and conditions - Introduction and key changes from the 1999 classification. *J. Periodontol.* 89, S1–S8.

51. Sachdeva, N., and Asthana, D. (2007). Cytokine quantitation: technologies and applications. *Front. Biosci.* **12**, 4682–4695.
52. Chiang, C.Y., Hsieh, M.L., Huang, K.W., Chau, L.K., Chang, C.M., and Lyu, S.R. (2010). Fiber-optic particle plasmon resonance sensor for detection of interleukin-1 $\beta$  in synovial fluids. *Biosens. Bioelectron.* **26**, 1036–1042.
53. Sánchez-Tirado, E., Salvo, C., González-Cortés, A., Yáñez-Sedeño, P., Langa, F., and Pingarrón, J.M. (2017). Electrochemical immunosensor for simultaneous determination of interleukin-1 beta and tumor necrosis factor alpha in serum and saliva using dual screen printed electrodes modified with functionalized double-walled carbon nanotubes. *Anal. Chim. Acta* **959**, 66–73.
54. Guerrero, S., Agüí, L., Yáñez-Sedeño, P., and Pingarrón, J.M. (2020). Design of electrochemical immunosensors using electro-click chemistry. Application to the detection of IL-1 $\beta$  cytokine in saliva. *Bioelectrochemistry* **133**, 107484.
55. Baraket, A., Lee, M., Zine, N., Sigaud, M., Bausells, J., and Errachid, A. (2017). A fully integrated electrochemical biosensor platform fabrication process for cytokines detection. *Biosens. Bioelectron.* **93**, 170–175.
56. Aydin, E.B., and Sezgintürk, M.K. (2018). A disposable and ultrasensitive ITO based biosensor modified by 6-phosphonohexanoic acid for electrochemical sensing of IL-1 $\beta$  in human serum and saliva. *Anal. Chim. Acta* **1039**, 41–50.
57. Cardoso, A.R., de Sá, M.H., and Sales, M.G.F. (2019). An impedimetric molecularly-imprinted biosensor for Interleukin-1 $\beta$  determination, prepared by in-situ electropolymerization on carbon screen-printed electrodes. *Bioelectrochemistry* **130**, 107287.
58. Choi, D.Y., Yang, J.C., Hong, S.W., and Park, J. (2022). Molecularly imprinted polymer-based electrochemical impedimetric sensors on screen-printed carbon electrodes for the detection of trace cytokine IL-1 $\beta$ . *Biosens. Bioelectron.* **204**, 114073.
59. Land, K.J., Boeras, D.I., Chen, X.S., Ramsay, A.R., and Peeling, R.W. (2019). REASSURED diagnostics to inform disease control strategies, strengthen health systems and improve patient outcomes. *Nature Microbiol.* **4**, 46–54.
60. Cennamo, N., Arcadio, F., Seggio, M., Maniglio, D., Zeni, L., and Bossi, A.M. (2022). Spoon-shaped polymer waveguides to excite multiple plasmonic phenomena: A multisensor based on antibody and molecularly imprinted nanoparticles to detect albumin concentrations over eight orders of magnitude. *Biosens. Bioelectron.* **217**, 114707.
61. Cennamo, N., Pesavento, M., and Zeni, L. (2021). A review on simple and highly sensitive plastic optical fiber probes for biochemical sensing. *Sensor. Actuator. B Chem.* **331**, 129393.
62. Cennamo, N., Massarotti, D., Conte, L., and Zeni, L. (2011). Low cost sensors based on SPR in a plastic optical fiber for biosensor implementation. *Sensors* **11**, 11752–11760.
63. Zeni, L., Perri, C., Cennamo, N., Arcadio, F., D'Agostino, G., Salmona, M., Beeg, M., and Gobbi, M. (2020). A portable optical-fibre-based surface plasmon resonance biosensor for the detection of therapeutic antibodies in human serum. *Sci. Rep.* **10**, 11154.
64. Guida, L., Bencivenga, D., Annunziata, M., Arcadio, F., Borriello, A., Della Ragione, F., Formisano, A., Piccirillo, A., Zeni, L., and Cennamo, N. (2023). An optical fiber-based point-of-care test for periodontal MMP-8 detection: A proof of concept. *J. Dent.* **134**, 104553.
65. Bencivenga, D., Arcadio, F., Piccirillo, A., Annunziata, M., Della Ragione, F., Cennamo, N., Borriello, A., Zeni, L., and Guida, L. (2023). Plasmonic optical fiber biosensor development for point-of-care detection of malondialdehyde as a biomarker of oxidative stress. *Free Radic. Biol. Med.* **199**, 177–188.
66. Cennamo, N., Piccirillo, A., Bencivenga, D., Arcadio, F., Annunziata, M., Della Ragione, F., Guida, L., Zeni, L., and Borriello, A. (2023). Towards a point-of-care test to cover atto-femto and pico-nano molar concentration ranges in interleukin 6 detection exploiting PMMA-based plasmonic biosensor chips. *Talanta* **256**, 124284.
67. Yeh, Y.J., Cho, C.J., Benas, J.S., Tung, K.L., Kuo, C.C., Chiang, W.H., Cho, J., Benas, J.-S., Tung, K.-L., Kuo, C.-C., and Chiang, W.-H. (2023). Plasma-Engineered Plasmonic Nanoparticle-Based Stretchable Nanocomposites as Sensitive Wearable SERS Sensors. *ACS Appl. Nano Mater.* **6**, 10115–10125.
68. Yeh, Y.J., Le, T.N., Hsiao, W.W.W., Tung, K.L., Ostrikov, K.K., and Chiang, W.H. (2023). Plasmonic nanostructure-enhanced Raman scattering for detection of SARS-CoV-2 nucleocapsid protein and spike protein variants. *Anal. Chim. Acta* **1239**, 340651.
69. Zubeidat, K., Jaber, Y., Saba, Y., Barel, O., Naamneh, R., Netanel, Y., Horev, Y., Eli-Berchoer, L., Shhadeh, A., Yosef, O., et al. (2023). Microbiota-dependent and -independent postnatal development of salivary immunity. *Cell Rep.* **42**, 111981.
70. Zhang, L., Xiao, H., and Wong, D.T. (2009). Salivary biomarkers for clinical applications. *Mol. Diagn. Ther.* **13**, 245–259.
71. Liu, J., Huang, D., Cai, Y., Cao, Z., Liu, Z., Zhang, S., Zhao, L., Wang, X., Wang, Y., Huang, F., and Wu, Z. (2022). Saliva diagnostics: emerging techniques and biomarkers for salivaomics in cancer detection. *Expert Rev. Mol. Diagn.* **22**, 1077–1097.
72. Huang, Z., Yang, X., Huang, Y., Tang, Z., Chen, Y., Liu, H., Huang, M., Qing, L., Li, L., Wang, Q., et al. (2023). Saliva - a new opportunity for fluid biopsy. *Clin. Chem. Lab. Med.* **61**, 4–32.
73. Melguizo-Rodríguez, L., Costela-Ruiz, V.J., Manzano-Moreno, F.J., Ruiz, C., and Illescas-Montes, R. (2020). Salivary Biomarkers and Their Application in the Diagnosis and Monitoring of the Most Common Oral Pathologies. *Int. J. Mol. Sci.* **21**, 5173.
74. Bostanci, N., Mitsakakis, K., Afacan, B., Bao, K., Johannsen, B., Baumgartner, D., Müller, L., Kotolová, H., Emingil, G., and Karpíšek, M. (2021). Validation and verification of predictive salivary biomarkers for oral health. *Sci. Rep.* **11**, 6406.
75. Miller, C.S., Ding, X., Dawson, D.R., 3rd, and Ebersole, J.L. (2021). Salivary biomarkers for discriminating periodontitis in the presence of diabetes. *J. Clin. Periodontol.* **48**, 216–225.
76. Blanco-Pintos, T., Regueira-Iglesias, A., Seijo-Porto, I., Balsa-Castro, C., Castelo-Baz, P., Nibali, L., and Tomás, I. (2023). Accuracy of periodontitis diagnosis obtained using multiple molecular biomarkers in oral fluids: A systematic review and meta-analysis. *J. Clin. Periodontol.* **50**, 1420–1443.
77. Ghassib, I., Chen, Z., Zhu, J., and Wang, H.L. (2019). Use of IL-1  $\beta$ , IL-6, TNF- $\alpha$ , and MMP-8 biomarkers to distinguish peri-implant diseases: A systematic review and meta-analysis. *Clin. Implant Dent. Relat. Res.* **21**, 190–207.
78. Gaba, F.I., Sheth, C.C., and Veses, V. (2021). Salivary biomarkers and their efficacies as diagnostic tools for Oral Squamous Cell Carcinoma: Systematic review and meta-analysis. *J. Oral Pathol. Med.* **50**, 299–307.
79. Cafiero, C., Spagnuolo, G., Marenzi, G., Martuscelli, R., Colamaio, M., and Leuci, S. (2021). Predictive Periodontitis: The Most Promising Salivary Biomarkers for Early Diagnosis of Periodontitis. *J. Clin. Med.* **10**, 1488.
80. Annunziata, M., Arcadio, F., Borriello, A., Bencivenga, D., Piccirillo, A., Stampone, E., Zeni, L., Cennamo, N., Della Ragione, F., and Guida, L. (2023). A novel plasmonic optical-fiber-based point-of-care test for periodontal MIP-1 $\alpha$  detection. *iScience* **26**, 108539.
81. Verdigué-Fernández, L., Arredondo-Hernández, R., Mejía-Estrada, J.A., Ortiz, A., Verdugo-Rodríguez, A., Orduña, P., Ponce de León-Rosales, S., Calva, J.J., and López-Vidal, Y. (2023). Differential expression of biomarkers in saliva related to SARS-CoV-2 infection in patients with mild, moderate and severe COVID-19. *BMC Infect. Dis.* **23**, 602.
82. Bencivenga, D., Stampone, E., Aulitto, A., Tramontano, A., Barone, C., Negri, A., Roberti, D., Perrotta, S., Della Ragione, F., and Borriello, A. (2021). A cancer-associated CDKN1B mutation induces p27 phosphorylation on a novel residue: a new mechanism for tumor suppressor loss-of-function. *Mol. Oncol.* **15**, 915–941.

## STAR★METHODS

### KEY RESOURCES TABLE

REAGENT or RESOURCE	SOURCE	IDENTIFIER
<b>Antibodies</b>		
recombinant antibodies anti- IL-1 $\beta$ [EPR21086]	Abcam	Cat# ab216995; Rabbit antibody; RRID: AB_2894877
<b>Biological samples</b>		
Healthy human saliva (for the dose-response curve)	periodontally healthy volunteer (aged 19)	N/A
Healthy human saliva	periodontally healthy volunteer (aged 69)	N/A
Pathological human saliva	periodontitis patient (aged 61)	In this work: sample1
Pathological human saliva	periodontitis patient (aged 62)	In this work: sample2
<b>Chemicals, peptides, and recombinant proteins</b>		
Recombinant human IL-1 $\beta$ protein (active)	Abcam	Cat# ab259387
Recombinant human IL-6 protein	Proteintech Group, Inc	Cat# HZ1019
Human IgA	Merck KGaA	Cat# 400109
Human IgG	Merck KGaA	Cat# 400122
Ethanol	Merck KGaA	Cat# 34852
N-Hydroxysuccinimide	Merck KGaA	Cat# 130672
N-(3-Dimethylaminopropyl)-N'-ethylcarbodiimide hydrochloride	Merck KGaA	Cat# 03449
( $\pm$ )- $\alpha$ -Lipoic acid (( $\pm$ )-1,2-Dithiolane-3-pentanoic acid)	Merck KGaA	Cat# T5625
Ethanolamine (2-aminoethanol)	Merck KGaA	Cat# E9508
Phosphate buffer saline (dipotassium; trisodium; dihydrogen phosphate; hydrogen phosphate; dichloride)	Merck KGaA	Cat# 524650
Bovine serum albumin	Merck KGaA	Cat# A3059
Tween 20 (2-[2-[3,4-bis(2-hydroxyethoxy)oxolan-2-yl]-2-(2-hydroxyethoxy)ethoxy]ethyl dodecanoate)	Merck KGaA	Cat# P1379
<b>Critical commercial assays</b>		
Simple Plex Human Multianalyte Assay	ProteinSimple™	custom (cartridge ID 247771; kit ID 225367)
<b>Software and algorithms</b>		
Spectra suite	Ocean insight	<a href="https://www.oceaninsight.com/support/software-downloads/">https://www.oceaninsight.com/support/software-downloads/</a>
OriginPro software	Origin Lab. Corp	<a href="https://www.originlab.com/try">https://www.originlab.com/try</a>
Simple Plex software	Protein simple	Provided with the ELLA system
Mathlab	MathWorks	<a href="https://it.mathworks.com/products/matlab.html">https://it.mathworks.com/products/matlab.html</a>

### RESOURCE AVAILABILITY

#### Lead contact

Further information and requests for resources and reagents should be addressed to the Lead Contact, A. Borriello ([adriana.borriello@unicampania.it](mailto:adriana.borriello@unicampania.it)).

#### Materials availability

This study did not generate new unique reagent.

### Data and code availability

- The datasets generated and analysed in this study will be shared by the [lead contact](#) upon request.
- This paper does not report original code.
- Any additional information required to reanalyze the data reported in this paper is available from the [lead contact](#) upon request.

## EXPERIMENTAL MODEL AND STUDY PARTICIPANT DETAILS

### Patient samples

5 mL of saliva each enrolled subject were collected at the Periodontology Unit of the Integrated Activity Care Department of Oral Surgery and Stomatology, Maxillo-facial Surgery and Rehabilitation of the University Hospital “Luigi Vanvitelli”. All the donors of saliva specimens participating to this “proof-of-concept” study were carefully selected on the basis of the following criteria: good systemic health, no drug assumption in the last three months, at least 20 teeth, no oral mucosal pathologies, no instrumental periodontal therapy, no antibiotic or antiseptic periodontal therapy. Drinking and eating was avoided for at least 2 h before the saliva collection. The study on saliva bio-specimens was approved by the Medical Ethics Committee (University of Campania “L. Vanvitelli”, Prot. 0016318/1, 05/26/2022) and performed in accordance with the Declaration of Helsinki. Written informed consent was obtained from all subjects prior to the participation in the study.

## METHOD DETAILS

### Chemicals and reagents

Recombinant human IL-1 $\beta$  protein (active form, 17,000 Da) was purchased from ABCAM (Cambridge, CB2 0AX, UK), together with recombinant antibodies anti-IL-1 $\beta$  [EPR21086], anti-IL-6 [EPR21711]. Recombinant human IL-6 protein (HumanKine) was purchased from Proteintech Group, Inc (Manchester, UK). Absolute ethanol, N-Hydroxysuccinimide (NHS), N-(3-Dimethylaminopropyl)-N'-ethylcarbodiimide hydrochloride (EDC), Lipoic acid, Ethanolamine (2-aminoethanol), PBS (dipotassium; trisodium; dihydrogen phosphate; hydrogen phosphate; dichloride) tablets, Tween 20 (2-[2-[3,4-bis(2-hydroxyethoxy)oxolan-2-yl]-2-(2-hydroxyethoxy)ethoxy]ethyl dodecanoate), human IgG and bovine serum albumin (protease- and globulin-free BSA) were purchased from Merck KGaA (Darmstadt, Germany). Human IgA were purchased from Origene Technology, Inc (Rockville, MD, USA). The cartridge for the Simple Plex Human Multianalyte Assay was from ProteinSimple (San Jose, CA, USA). The PBS solution was obtained by dissolving tablets in Milli-Q water to yield 10 mM phosphate buffer, 140 mM NaCl, and 3 mM KCl, pH 7.4. All other chemicals were diluted by using Milli-Q water or PBS solution, as reported in the text. All the reagents were at the maximum of purity and all the solutions were prepared and filtered just before the use.

### SPR optical fiber sensor system

The plasmonic probe used to detect the analyte of interest is based on a modified plastic optical fiber, monitored by a simple experimental setup. In particular, the used POF probe has been obtained by three low-cost manufacturing steps, in order to excite the SPR phenomenon in a planar sensing region 1 cm long, as thoroughly described in.<sup>65</sup> In detail, we employed the SPR phenomena to monitor the antigen (analyte)/antibody binding through the use of a plastic optical fiber (POF) with a core in poly(methylmetacrylate) or PMMA (diameter = 980  $\mu$ m). In detail, starting from a classical POF fixed in a specific resin block, we obtained a D-shaped POF region through polishing procedures. Following that, a multilayer was created on the D-shaped POF planar sensing surface using spin coater and sputter coater equipment. As detailed in Cennamo N. et al.,<sup>62</sup> a photoresist buffer layer having a refractive index greater than the core of the POF was placed between the POF core and a gold nanofilm in order to increase optical responsiveness. Lastly, by using the chemistry of lipoic acid/N-Hydroxysuccinimide/N-(3-Dimethylaminopropyl)-N'-ethylcarbodiimide hydrochloride, the receptorial self-assembled monolayer was made on the plasmonic surface as detailed in the next paragraph.

### Functionalization of SPR-POF plasmon surfaces and immunofluorescence

The plasmon surface was functionalized essentially as previously reported by Zeni and colleagues in 2020,<sup>63</sup> and appropriately modified as in.<sup>64–66</sup> Briefly, the POF plasmon surfaces were washed 3 times with Milli-Q water (5 min each), and similarly 3 times with 8% ethanol in Milli-Q water. Subsequently, an incubation of 18 h with 0.3 mM lipoic acid in 8% ethanol was performed, allowing surface coating with the exposed carboxyl groups. The coated POF surfaces were activated by incubation for 20 min with 200 mM N-Hydroxysuccinimide/50 mM EDC (NHS/EDC) in phosphate buffered saline, pH 7.4 (PBS) and, thereafter, washed 3 times with PBS. The anti-IL-1 $\beta$  antibody was covalently immobilized on the activated surfaces by 2 h incubation with 10  $\mu$ L of anti-IL-1 $\beta$  (ab216995) (0.5  $\mu$ g/ $\mu$ L). Subsequently, the SAM was washed 3 times with PBS to remove the excess of the unbound antibody; finally, the non-reacted sites on the monolayer were deactivated by leaving the biosensing surface in 1 M ethanolamine buffer, pH 8.0, for 30 min. The whole procedure was performed at room temperature and, at each step, the surfaces were first dried under a gentle nitrogen stream. Finally, the functionalised platforms were rinsed thoroughly and stored at 4°C in PBS only if used the day after or, alternatively, in PBS/0.01% Sodium azide (NaN<sub>3</sub>) to prevent microbial contamination during long-term storage. For the 3D characterization and the evaluation of primary antibody distribution, we used the immunofluorescence technique: briefly, coverglasses (diameter = 1 cm; thickness = 0.13 mm) were covered with a gold nanofilm (thickness = 25 nm) and functionalised as the presented biosensor. The primary antibody against IL-1 $\beta$  was added only in a half of the glass



surface, to discriminate on the same glass the antibody fluorescence signal from the background. Then, as reported in Bencivenga et al., 2021,<sup>82</sup> the secondary antibodies (conjugated with Alexa Fluor 647 fluorochrome) were incubated for 1 h at room temperature in the dark, covering all the glass surface and, then, they were washed and transferred on slices with a coverslip sealant. Almost 3 different fields were analyzed by using ECLIPSE Ti2 inverted microscope/60× plan apo oil objective (1.40 NA)/DS-Qi2 camera and a representative image is reported in [supplementary materials](#) section (Figure S1).

### IL-1β binding test in buffer solution and saliva and specificity and stability test

Serial dilutions of human recombinant IL-1β in PBS (from 25 to  $4 \times 10^3$  p.m.) were prepared; then, 50 μL of each dilution were dropped on the sensing region of the SPR-POF sensor and incubated for 3 min, to allow the binding with the immobilized anti-IL-1β antibody. After each incubation step, a wash with PBS was performed, and the related SPR spectrum was obtained by normalizing the transmitted spectrum of IL-1β solution to a reference spectrum obtained in air (where the plasmonic resonance is not excited) and comparing to a blank (PBS only). Thus, only the shift in resonance wavelength caused by the specific recognition was determined. All steps were performed at room temperature. The Langmuir model was used to calculate the LoD, the affinity constant ( $K_{aff}$ ), and the sensitivity at low concentrations. To test the specificity of the detection, the same procedure was followed to analyze PBS solutions containing BSA (1 nM), human recombinant IL-6 (1 nM), IgG (1 nM) and IgA (1 nM and 600 nM): the wavelength variations ( $\Delta\lambda$ ) were calculated with respect to the blank (buffer only) and compared to that related to the measurement of 1 nM IL-1β solution.

The IL-1β detection efficiency was also evaluated in saliva. In detail, a sample of saliva from a healthy volunteer (aged 19) was collected at the Periodontology Unit of the Integrated Activity Care Department of Oral Surgery and Stomatology, Maxillo-facial Surgery and Rehabilitation of the University Hospital “Luigi Vanvitelli”. The healthy donor was carefully selected on the basis of the criteria listed in the [STAR methods](#), “[experimental model and study participant details](#)” section. The healthy saliva was harvested in sterile tubes enriched with protease inhibitors’ cocktail, diluted 1:50 with PBS and immediately used to prepare serial dilutions of IL-1β (from 25 to  $4 \times 10^3$  pM). Then, the samples were analyzed as reported above and, again, the Langmuir model was exploited to calculate the LoD,  $K_{aff}$ , and sensitivity at low concentrations in saliva. Furthermore, by using both calibration curves (in PBS and in saliva), the ranges of proportionality, Pearson correlation coefficient and  $R^2$  were calculated using OriginPro software (Origin Lab. Corp, Northampton, MA, USA).

The stability of the proposed device was tested after 6 weeks from functionalization and/or at low pH. In detail, three SPR surfaces were contemporaneously and equally functionalized with anti-IL-1β antibodies. 25 pM IL-1β solution was used for all the subsequent measures. 5 min of incubation with 100 mM Glycine-HCl, pH 2.2, were used to test the stability at low pH and as a potential regeneration strategy of the sensing SAM. These biosensors were used as schematized in [Figure S2](#), and the experiments were performed in triplicates. Finally, the measured  $\Delta\lambda$  obtained for each condition were compared with their proper controls.

### Determination of salivary IL-1β concentration in periodontitis saliva

IL-1β was measured directly in saliva samples from a periodontally healthy subject and a periodontitis patient, chosen according to the case definitions and the classification of periodontal diseases reported in Caton et al., 2018. Specifically, the two subjects were enrolled in the study at the Periodontology Unit of the Integrated Activity Care Department of Oral Surgery and Stomatology, Maxillo-facial Surgery and Rehabilitation of the University Hospital “Luigi Vanvitelli”, according to the protocol (Prot. 0016318/i of May 26, 2022) approved by the Institutional Review Board. They were both Caucasian males, aged 69 (the periodontally healthy subject) and 61 (the periodontitis patient). The selection criteria included good systemic health, no drug assumption in the last three months, at least 20 teeth, no oral mucosal pathologies, no instrumental periodontal therapy, no antibiotic or antiseptic periodontal therapy. Drinking and eating was avoided for at least 2 h before the saliva collection. The subjects provided 5 mL of saliva. Protease inhibitors’ cocktail was quickly added to the samples. The specimens were diluted 1:2 with PBS just before the analyses on POF and immediately analyzed, or, alternatively stored as aliquots at  $-80^\circ\text{C}$ . For measurements, the spectra were recorded after 3 min of incubation of saliva with the SAM, and each measure was performed in triplicate and expressed in terms of mean  $\pm$  standard deviation.

The calculated IL-1β concentrations were compared to those derived from Ella system (ProteinSimple, San Jose, CA, USA) analyses performed on the same samples, according to the manufacturer instructions. Briefly, a 2-fold dilution of each saliva sample was spun for 20 min at  $1000 \times g$  and  $4^\circ\text{C}$ , then added to the cartridge. Subsequently, the cartridge was quickly inserted into the reader and run for about 90 min at RT, and the IL-1β levels were obtained by interpolation from the calibration curve and expressed as pg/mL. Finally, considering the molecular weight of the interleukin active form (17,000 Da), the concentrations have been expressed and reported in molarity.

Another sample (sample 2) was examined in order to see whether the matrix components affect measurements. It was obtained from a second 62-year-old periodontitis patient who met the criteria for enrollment in this study. In order to determine the quantities of the cytokine in samples 1 and 2 (diluted 1:2 and 1:10 respectively) for the test of background noise, wavelength shifts on both dose-response curves in PBS and in saliva were interpolated. Then, the estimated concentrations on both curves were compared.

### QUANTIFICATION AND STATISTICAL ANALYSIS

In the dose-response curves and Langmuir fittings of the collected data, the wavelength variations ( $\Delta\lambda$ ) related to the reported IL-1 $\beta$  concentrations represent the mean values of three different measurements. The error bars (reported in the fitting curves and in the specificity test) correspond to the major value of the calculated standard deviations. The OriginPro software (Origin Professional, Origin Lab. Corp, Northampton, MA, USA) was used to obtain the Langmuir fitting of the experimental values and the statistical parameters, Pearson correlation coefficient and  $R^2$ . The IL-1 $\beta$  concentrations in healthy and periodontitis patient saliva samples were determined by interpolation on the dose-response curve and origin from the mean values of three measurements on the same biospecimens.